Refill Strategy for Two-Tank Cold Gas Propulsion Systems

Samuel Wood*
Georgia Institute of Technology, Space Systems Design Lab, Atlanta, GA, 30332

Cold gas propulsion systems using a saturated liquid-vapor mixture as propellant often use separate tanks for storage and actuation. The pressure of a plenum is regulated via refills from a storage tank. Without a propellant management device, simple pressure-controlled refills can inject unwanted liquid into the plenum. This phenomenon leads to unpredictable thrust and a lower-than-expected specific impulse. These undesirable characteristics are mitigated by using a model-based closed-loop refill strategy. A valve flow equation is combined with system characterization data to approximate the average mass flow between the storage tank and plenum. Refill valve opening and closing times are controlled to allow the system to reach steady state prior to refilling or actuating. Controller operation is tested and validated on integrated cold gas systems in orientations that allow either liquid or gas to be in contact with the plenum refill port. These simulated worst-case and best-case on-orbit conditions are tested across the system's full temperature operating range. This paper describes the model development, integrated hardware testing, and improved system performance associated with the model-based plenum refill strategy. These findings enable two-tank cold gas propulsion systems using pressure-controlled refilling to deliver more repeatable system operation.

I. Nomenclature

$GLRG$	=	Glenn Lightsey Research Group
$SSDL$	=	Space Systems Design Laboratory
$CGPS$	=	Cold Gas Propulsion System
$SunRISE$	=	Sun Radio Interferometer Space Experiment
$SWARM\text{-}EX$	=	Space Weather Atmospheric Reconfigurable Multiscale Experiment
$VISORS$	=	Virtual Super Optics Reconfigurable Swarm
CLF	=	Closed Loop Fire
CLR	=	Closed Loop Refill
I_{sp}	=	Specific Impulse
$MDNAV$	=	Mission Design and Navigation
GNC	=	Guidance, Navigation, and Control
ADC	=	Analog to Digital Converter

*Graduate Research Assistant - Georgia Institute of Technology, Department of Aerospace Engineering, Atlanta, GA, 30332

II. Introduction

The Glenn Lightsey Research Group (GLRG) in Georgia Tech's Space Systems Design Laboratory (SSDL) is currently developing cold gas propulsion systems (CGPS) for the SunRISE, SWARM-EX, and VISORS formation flying missions (Figure 1) [1] [2] [3]. The design for these units is built upon former GLRG projects such as the CGPS for Biosentinnel and ASCENT [4] [5]. These two-tank cold gas systems use additively manufactured structures that are designed to fit in a small volume. This enables the CGPS to be used for ΔV and desaturation maneuvers on volume-restricted CubeSat missions. The application of these systems to formation flying requires performance to be well characterized and predictable. The performance of current systems has been improved by implementing a data-defined model-based refill strategy that ensures operation is consistent given the physical limitations of a GLRG CGPS.

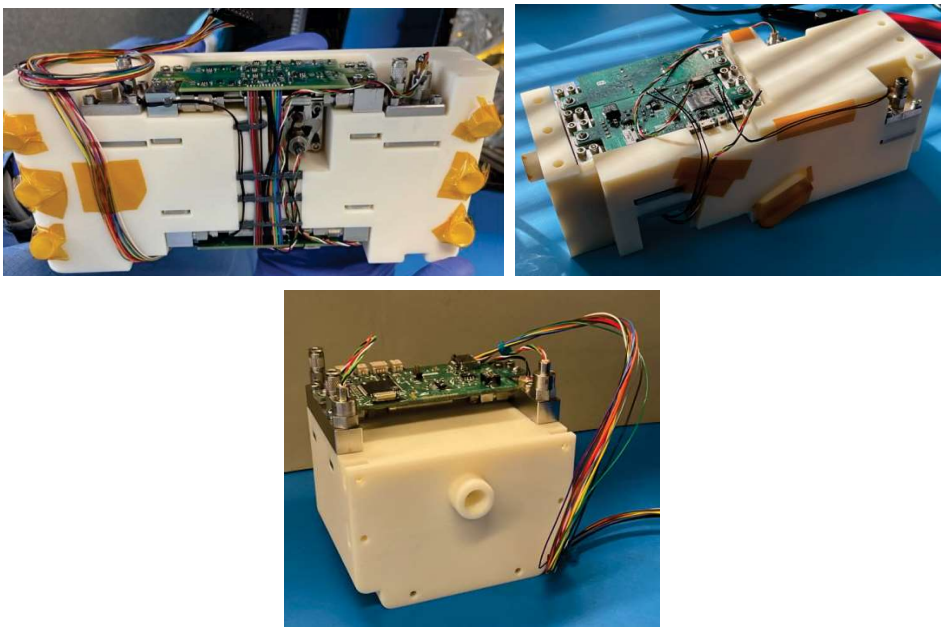

Fig. 1 Current GLRG propulsion systems (Left) SunRISE [6], (Right) VISORS [7], (Bottom) SWARM-EX [7]

A. Two-Tank Systems

In the GLRG CGPS design a main tank stores propellant and a plenum is used for actuation. The two tanks are connected via internal flow paths and a valve. The plenum vents gaseous propellant through nozzles that are also connected via internal flow paths and valves [8]. A diagram of a simplified CGPS can be seen in Figure 2.

A saturated liquid-vapor mixture of R-236fa is contained in the main tank. The plenum is intended to be refilled with gaseous propellant. To ensure that the plenum is filled with gas, it is limited to a high refill bound defined as a fraction of the main tank pressure. Typically, during operation, this high refill bound is set to 90%.

The saturation properties of R236-fa are outlined in Table 1 [9]. This table reflects the temperature-pressure

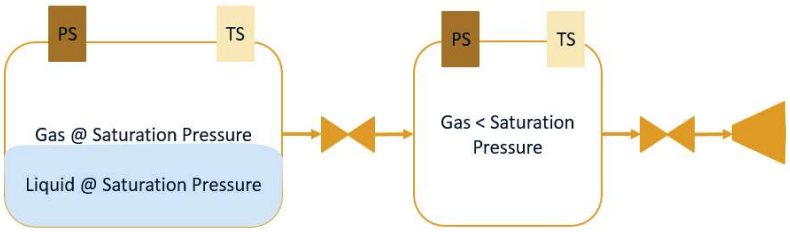

Fig. 2 Diagram of a simplified CGPS

relationship for the saturated propellant at the expected nominal and extreme system temperatures. Pressure cannot be directly controlled in the main tank, meaning both main tank and plenum pressures vary with temperature. Thrust is significantly impacted by the system temperature, and to maintain reasonable thrust magnitudes, the plenum is limited to a low refill bound [5]. The plenum is considered depleted when the pressure drops below this low bound, typically defined as 80% of the main tank pressure. Thrust performance modeling of a single nozzle firing into a vacuum is shown in Figure 3 [4].

Temperature [$°C$]	Saturation Pressure [psi]
-20	6.31
20	33.3
50	84.7

Table 1 Saturation properties of R236-fa [9]

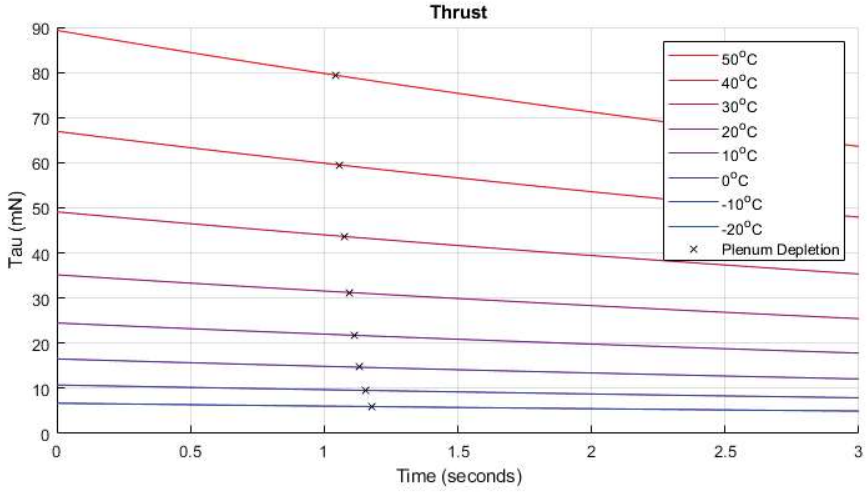

Fig. 3 Firing operation at different temperatures for GLRG CGPS [4]

B. Operation

Pressure transducers and thermistors are used to monitor tank pressures and temperatures as indicated in Figure 2. During operation, if a nozzle is fired, the plenum pressure drops as gas exits. When the pressure drops below the low refill bound, all nozzle valves are closed and a refill begins. This is what is referred to as closed-loop firing (CLF) and closed-loop refilling (CLR). A CLF command instructs the system to open one or more nozzle valves for a specified amount of time. Long-duration firing is split up by a series of refills. Figure 4 shows the theoretical plenum pressure vs. time plot for a CLF command. Refills are intended to maintain the pressure in the plenum between the two refill bounds.

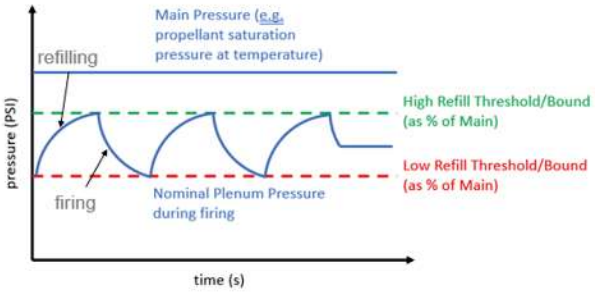

Fig. 4 Theoretical refill operation

During the testing of a propulsion system engineering development unit (EDU), the issue of liquid entering the plenum was discovered [6]. Unexpected saturation of a thrust stand during performance testing revealed that liquid could be expelled from the nozzles during extended firing operations. Subsequent testing of continuous firing and refilling revealed that the plenum pressure continues to rise after the refill valve is commanded closed. The thrust stand saturation indicates a significantly higher mass flow rate out of the plenum than expected. The rising pressure after the refill valve is closed indicates that a phase transition from liquid to gas is occurring in the plenum.

The liquid in the plenum introduces two operational risks to a mission. The first is an unpredictable thrust when liquid is ejected from the nozzle. This is a large risk for formation flying missions that require precise knowledge of thrust for operation [3]. The second is a reduced specific impulse (I_{sp}) which negatively impacts the expected mission lifetime. The goal of this work is to mitigate the risks associated with liquid entering the plenum during operation. The following sections outline the development of a data-defined model and steady-state determination algorithm for refilling. Details of refill operation, characterization testing, and refill validation on hardware show the results of an updated refill strategy.

III. Refill

A successful refill means actuating the refill valve to raise the plenum pressure to the predefined high threshold. When the system is commanded to do a CLR, it checks its current plenum pressure. A refill cycle begins if the pressure is less than the high refill threshold. The refill stops when the plenum pressure is greater than or equal to the high

threshold. At this point, the system enters a normal operating state where nozzle fires can be commanded. It is important to note that when a refill is complete, operators have commanded the system to reach a plenum pressure equal to the high threshold. For Mission Design and Navigation (MDNAV) and Guidance, Navigation, and Control (GNC) this is a fundamental operational assumption. Any gross overshoot can lead to problems for both pre-defined and closed-loop maneuvers.

For a single nozzle fire that starts with a full plenum, the depletion time is 1.1 seconds. This time varies slightly with temperature and can be seen in Figure 3 for the SunRISE system. Plenum volume also impacts the depletion time, but the plenum is a relatively consistent volume across the three projects. Any burn longer than 1.1 seconds is broken up by a series of refills. Large ΔV maneuvers are divided into 1.1 second increments by refills, extending the time it takes to perform a maneuver. Longer refill times mean significantly longer burns to achieve the same total ΔV. The following sections explain the refill logic and motivate the need for accurate predictions of mass entering the plenum as a function of various state variables to ensure predictable operation.

A. Original Refill Strategy

1. Logic

The original system operation followed the logic seen in Figure 5. It simply commands the refill valve to open until the high threshold is met. This is designed with the assumption that gas is entering the plenum and there are no transients in the system caused by liquid vaporization. The performance of this refill displays the issues with this logic.

2. Performance

Analyzing the plenum pressure data from testing revealed gross overshoots after long-duration burn-refill cycles. The example in Figure 6 shows that it took almost 20 minutes for the plenum pressure to reach a final steady-state value. While the total refill times are small, on the order of five to ten seconds, each cycle introduces more liquid into the plenum. As the long-duration nozzle firing continues, the risk of ejecting liquid increases.

This testing also reveals the fact that orientation plays a role in the performance of the refill [6]. With a main tank partially filled with propellant, different orientations lead to different refill behaviors. This is due to the fact that in some orientations the gas bubble in the main tank interfaces with the entrance to the refill flow path. In these situations, the original refill strategy behaves as intended. Doing this testing in a 1g environment means that the location of the main tank's gas bubble can be controlled. However, in a microgravity environment, the location of the gas bubble is uncontrollable and unknown. While it is a function of variables such as tank temperature gradients and system acceleration, it is reasonable to assume that the liquid will be sticking to the walls and internal passages on orbit due to surface tension [10]. Even as liquid depletes in the main tank during a mission's lifetime, and the bubble size increases, the risk of injecting liquid into the plenum is still present.

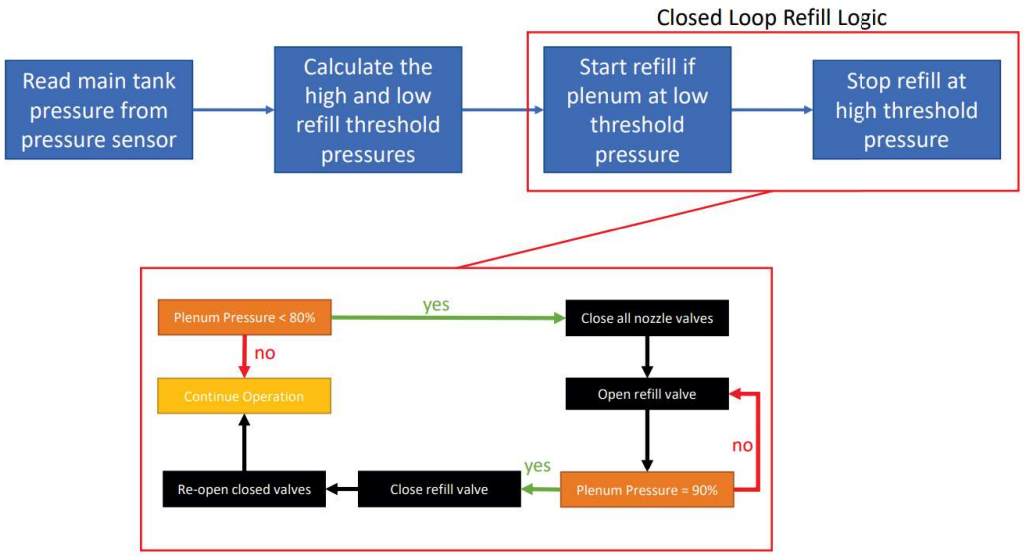

Fig. 5 Original refill operation logic

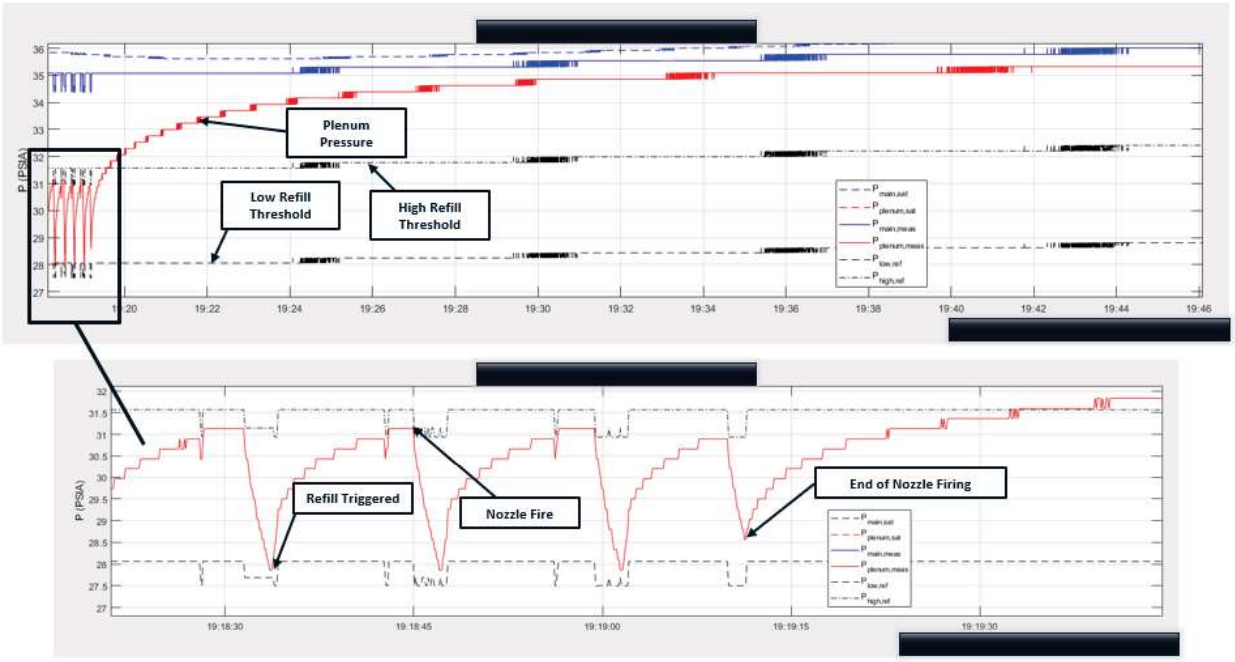

Fig. 6 Overshoot during original refill operation

B. Fixed-Duty Refill Strategy

Testing done on the original refill strategy motivated a change in refill strategy logic. The first concept explored is a fixed-duty refill cycle wherein the refill valve would be held closed for t_s milliseconds (cycle off time) immediately following a pulse of t_p milliseconds (cycle on time). The intention is to allow each of the t_p millisecond pulses to settle before introducing any additional liquid into the plenum. Waiting for the liquid to vaporize ensures that all of the refill

risks are minimized. Fixed refill duty cycles continue until the high threshold is met.

1. Logic

Previously, the refill valve would be open for a total of five to ten seconds. Testing this new logic, the refill valve can be opened for as little as 50 milliseconds at a time to conservatively monitor the rise in plenum pressure. The valve open portion of the duty cycle must be kept small to avoid any gross overshoot when the plenum pressure is close to the high threshold. Through testing, it was found that the valve closed portion of the duty cycle, t_s, must be 3000 milliseconds for every 50 milliseconds of valve open time, t_p, to passively allow the plenum pressure to reach a steady state. Figure 7 shows the fixed-duty refill cycle successfully reaching the desired high threshold without overshooting.

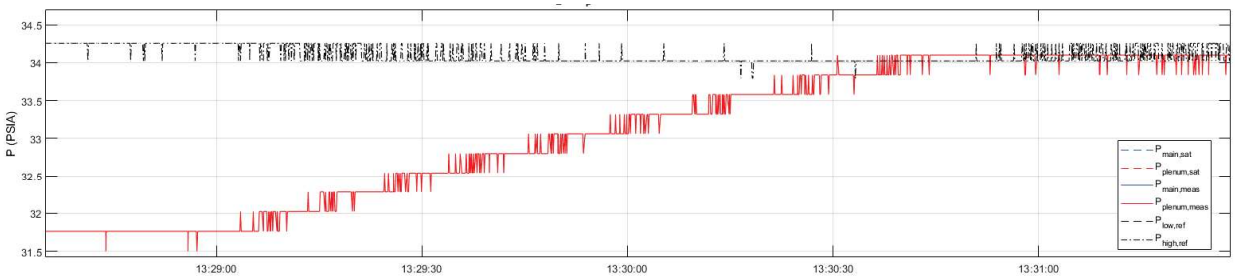

Fig. 7 fixed-duty refill results

2. Performance

The results in Figure 7 are an example of a fixed-duty refill cycle at an ambient temperature. This example shows a refill going from 83.5% to 90% of the main tank pressure. This refill takes 90 seconds. Refills from the standard 80% to 90% can take up to 150 seconds at ambient temperatures. This is 15-30 times longer than the original refill times. For impulsive maneuvers broken up by refills, it would take more than an hour for 25 seconds of nozzle firing. The fixed-duty refill logic is a good proof of concept that plenum pressure can be controlled to reach a desired final steady-state pressure, but improvements must be made to the refill timing for the systems to operate with a reasonable firing-refilling duty cycle.

C. Data-Defined Model-Based Refill Strategy

The results from the fixed-duty refill strategy motivated the concept of the model-based refill strategy. Similar logic will be employed wherein the refill valve is held closed immediately following a pulse of t_p milliseconds, but the on and off times (t_p and t_s) for the duty cycle are not fixed. Instead, the refill valve pulse time, t_p, comes from a model that predicts the amount of mass needed to raise the plenum pressure to the high threshold. The settling time, t_s, is then actively determined by monitoring the transients of the resulting pulse, waiting for the plenum pressure to reach a steady state.

Additionally, the new strategy must predict t_p across a broad range of operating temperatures. As displayed in Table 1, the pressure values in the main tank are significantly different within the operational temperature range. This has an impact on the states of the systems and must be accounted for in the new refill strategy.

For predicting t_p, the model-based refill strategy uses valve flow equations [11] and the ideal gas law to calculate the mass flow rate between the tanks and the amount of mass needed in the plenum, respectively, at a known initial state. Determining t_s comes from sampling the plenum pressure in discrete time steps and taking a running average pressure and running average rate of change. When the two values fall within a predefined threshold, the refill cycle is complete. The intention is to be able to command a t_p at any given initial state and have it reach the high threshold at a steady state in an actively determined time, t_s.

IV. Model Development

A. Determining the Steady State Plenum Pressure

1. Theory

Determining when a refill pulse reaches a steady state relies on sampling the plenum pressure at fixed intervals after a refill pulse, t_p, has been completed. The logic tracks the current plenum pressure and previous plenum pressure readings to determine a running average pressure and rate of change. These averages are calculated as moving means. The microcontroller integrated in the CGPS electronics only tracks the average of the previous n samples. This is important so that the steady state determination is independent of the magnitude of pressure change in the plenum. If all samples taken after the refill pulse are used to calculate the moving means, larger pressure increases would cause the mean to converge significantly more slowly to the steady state value. The following variables in Table 2 define the states of the plenum that are used to determine whether the pressure has reached a steady state. The pressure units are in psi as the onboard calibration function outputs readings in psi.

Variable	Description	Units
n	# of samples for the moving average	$samples$
f	sampling frequency	Hz
T	sampling window	s
$P_{p,k}$	kth plenum pressure sample after refilling	psi
$\Delta P_{p,k}$	$P_{p,k}$ rate of change	$\frac{psi}{s}$
$\bar{P}_{p,k}$	average plenum pressure at kth sample	psi
$\Delta \bar{P}_{p,k}$	average rate of change at kth sample	$\frac{psi}{s}$
$P_{p,t}$	plenum pressure steady-state tolerance	psi
$\Delta P_{p,t}$	rate of change steady-state tolerance	$\frac{psi}{s}$

Table 2 Variable definitions for steady state determination logic

From these variables, the relationship between the running averages of the plenum pressure and rate of change can be defined. Discrete variables are sampled at a frequency, f. The number of samples for the moving average, n, is defined as a function of the window size, T. The sampling frequency and window size are parameters that can be tuned to impact the algorithm's performance.

$$n = fT \tag{1}$$

When the controller has fewer than n samples, $n = k$. Otherwise, n is fixed as defined in equation (1). The following is a simple definition of the average plenum pressure of the current state and the future state.

$$\bar{P}_{p,k} = \sum_{j=1}^{k} \frac{P_{p,j}}{n} \tag{2}$$

$$\bar{P}_{p,k+1} = \sum_{j=1}^{k+1} \frac{P_{p,j}}{n+1} \tag{3}$$

When a new sample is collected, the previous average, $\bar{P}_{p,k}$, is already known. To minimize the number of floating point operations needed to calculate the average, equation (3) is simplified as follows using equation (2)

$$\bar{P}_{p,k+1} = \frac{\bar{P}_{p,k} n + P_{p,k+1}}{n+1} \tag{4}$$

Substituting in equation (3) for $k = k - 1$ the current running average plenum pressure can be calculated with knowledge of the previous running average

$$\bar{P}_{p,k} = \frac{\bar{P}_{p,k-1}(n-1) + P_{p,k}}{n} \tag{5}$$

This means the only variable needed to update $\bar{P}_{p,k}$ is $P_{p,k}$ as the number of samples, n, is either fixed or equal to k. A relationship for the rate of change can be defined using similar logic and the following computation for the rate of change between two samples.

$$\Delta P_{p,k} = f(P_{p,k} - P_{p,k-1}) \tag{6}$$

$$\Delta \bar{P}_{p,k} = \frac{\Delta \bar{P}_{p,k-1}(n-1) + \Delta P_{p,k}}{n} \tag{7}$$

Given equation (7), to calculate $\Delta \bar{P}_{p,k}$ the controller only needs knowledge of $P_{p,k}$ and $P_{p,k-1}$.

The final parameters that need to be defined are the tolerances to determine when a steady state is reached. These numbers are defined using information about the pressure calibration functions. Pressure values come from a calibration function that samples and converts ADC readings to psi. The sensitivity of the ADC to P function is a known value. The most precise approximation of a steady-state signal occurs when the running average lies within 1 bit of the current raw

ADC reading. For this reason, the plenum pressure steady-state tolerance, $P_{p,t}$, is half of the sensitivity. As an example, the SunRISE EDU2 plenum pressure calibration function has a sensitivity of 0.234 $\frac{psi}{bit}$ meaning the $P_{p,t}$ value is 0.117 psi. The average plenum pressure portion of the steady-state condition is met when the following condition is true.

$$\bar{P}_{p,k} - P_{p,t} \leq P_{p,k} \leq \bar{P}_{p,k} + P_{p,t} \tag{8}$$

The tolerance for the rate of change has a similar motivation. If the current rate of change is approximately equal to zero and condition (8) is also met, one can confidently say that the plenum pressure has reached a steady state. For this reason, $\Delta P_{p,t}$ is set equal to 0.01 psi, and the steady state condition is met when the following is true.

$$\Delta\bar{P}_{p,k} \leq \Delta P_{p,t} \tag{9}$$

The final part of this algorithm is the initialization of the averages. The initial average plenum pressure, $\bar{P}_{p,0}$, is set equal to the value from the first sample. The initial rate of change, $\Delta\bar{P}_{p,0}$, is set equal to the rate of change between the first two samples. To avoid the steady state conditions being met too early, the controller samples and propagates averages for three seconds before the steady state condition can be met.

2. Implementation

Given the equations above, this algorithm is simulated in MATLAB. The state of the propulsion system is simulated as a function of temperature. Refills are simulated using an overdamped step function starting at the low refill threshold and ending at the high refill threshold. The signal is sampled to reflect the discretization that occurs when ADC values are converted to pressure readings. The strategy is also tested with noise in the signal to ensure that it still operates as expected. A function is used to randomly add ±1 bit to the raw input signal. A uniform distribution is discretized to calculate the noise magnitude of 0, 1, or -1 bit. This emulates behavior that can be seen in Figure 7 when pressure readings jump between a single bit as the reading comes to a steady state.

Figure 8 shows example refills across the full temperature range. The point plotted on the step function indicates when the algorithm determines a steady state is reached. The dotted lines are the respective high and low refill thresholds for each pulse. The simulated step function settling time is set to 30 s. Deviations from this 30 s input are an artifact of the ADC discretization and the 0.25 psi sensitivity. Using this simulation, the optimal sampling frequency, f, and window size, T, are set to 2 Hz and 5 s for refills that take between 30 to 60 s to settle.

B. Refill Valve Pulse Time Model

For the refill valve pulse time model, the ideal gas law and valve flow rate equations are used [11]. The intention is to approximate the mass flow rate between the main tank and plenum, predict the amount of mass needed to get the

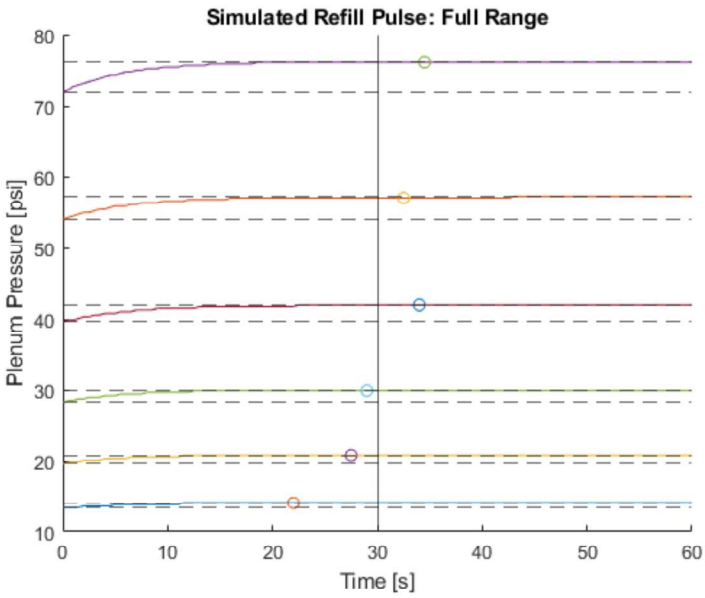

Fig. 8 Refill pulse steady state determination across the full operating range

plenum to the high threshold and command a pulse time to inject the predicted mass given the calculated mass flow rate. This modeling is intended to be a first-order approximation of the behavior of a refill pulse. In reality, two-phase flow equations would more precisely capture the system's pressure dynamics. The first-order approximation is intended to be used with experimental data to form a data-defined prediction for t_p. The following variables in Table 3 define the states of the propulsion system and the constants that will be used in this model.

Variable	Description	Units
t_p	refill valve pulse time	s
$\dot{m}_{ave}$	average mass flow rate between tanks	$\frac{kg}{s}$
C_v	valve flow coefficient	
ρ_w	density of water at STP	$\frac{kg}{m^3}$
ρ_p	density of liquid propellant at current temperature	$\frac{kg}{m^3}$
P_m	main tank pressure	Pa
$P_{p,i}$	initial plenum pressure	Pa
Δm	change in plenum mass	kg
$P_{p,f}$	final plenum pressure	Pa
V	plenum volume	m^3
R	gas constant	$\frac{J}{kgK}$
T	plenum temperature	K
c	data-defined valve flow parameter	

Table 3 Variable definitions for refill pulse time model

The first governing equation gives the average mass flow rate between the main tank and plenum given the initial

state before refilling. This equation uses a worst-case assumption of liquid entering the plenum. Liquid injection is a worst-case assumption as this will give the highest average mass flow rate between the two tanks. Additionally, the mass flow rate will decrease as the plenum pressure increases. Using the initial plenum pressure to calculate the mass flow rate will give an estimate that is practically higher than the expected average. Assuming a high mass flow rate means that the relative refill pulse time predictions will be lower, minimizing the risk of overshooting the final plenum pressure

$$\dot{m}_{ave} = C_v \rho_w \sqrt{\rho_p (P_m - P_{p,i})} \tag{10}$$

To calculate the amount of mass needed to inject into the plenum, the ideal gas law is used. Note that the final plenum pressure defined here is set to the high threshold by the controller.

$$\Delta m = \frac{(P_{p,f} - P_{p,i})V}{RT} \tag{11}$$

$$\frac{\Delta m}{t_p} = \dot{m}_{ave} \tag{12}$$

Assuming that the average mass flow rate can be represented using equation (11)'s change in mass and the refill pulse time, equation (10) and equation (12) can be equated to get the following relationship

$$\frac{(P_{p,f} - P_{p,i})V}{RTt_p} = C_v \rho_w \sqrt{\rho_p (P_m - P_{p,i})} \tag{13}$$

Equation (13) can be rearranged to isolate t_p as follows

$$t_p = \frac{RTC_v \rho_w}{(P_{p,f} - P_{p,i})V} \sqrt{\rho_p (P_m - P_{p,i})} \tag{14}$$

Equation (14) is the basis for modeling the refill pulse. As mentioned, this equation will more accurately predict t_p given experimental data. This helps include system dynamics that may not be captured by the simple approximations assumed in equations (10) and (11).

While the model is simple, it still has an unknown parameter on the right-hand side of the equation, C_v. This is the valve flow coefficient that is typically assumed to be constant and is provided by the valve manufacturer. In the integrated propulsion systems, though, the valve is in line with filters and flow paths. This makes the true "flow coefficient" between tanks more complicated. Experiments can be designed to calculate this parameter given all of the other state information. System characterization testing must collect data such that the following equation is satisfied

$$f(P_m, P_{p,i}, P_{p,f}, T) = c = \frac{1}{C_v} = \frac{RT\rho_w}{(P_{p,f} - P_{p,i})Vt_p} \sqrt{\rho_p (P_m - P_{p,i})} \tag{15}$$

After data is collected, the calculated value for c in equation (6) can be approximated using regression where the regressors are known state variables of the system. This function of known values can be plugged back into equation (5) to get a relationship for t_p with no unknowns on the right-hand side of the equation. The final form of equation (5) then becomes

$$t_p = \frac{RT\rho_w f(P_m, P_{p,i}, P_{p,f}, T)}{(P_{p,f} - P_{p,i})V}\sqrt{\rho_p(P_m - P_{p,i})} \tag{16}$$

The following section describes the design, operation, and results of the system characterization testing.

C. System Characterization Testing and Data Reduction

Characterization testing was designed to be run on SunRISE EDU2. The EDU is put in an orientation that forces liquid into the plenum and a test sequence is run to collect characterization data for liquid refills. Testing is run in a thermal vacuum chamber. As the goal is to satisfy equation (15) and perform regression to find $f(P_m, P_{p,i}, P_{p,f}, T)$, the following test sequence was defined.

1) Start at an initial plenum pressure, $P_{p,i}$
2) Command a refill pulse of length, t_p
3) Wait for the refill pulse to reach a steady state value, $P_{p,f}$
4) Vent the plenum and return to the initial plenum pressure, $P_{p,i}$
5) Repeat steps (1 - 4) for varying values of $P_{p,i}$ and t_p
6) Repeat steps (1 - 5) for different temperature setpoints, T

Independent Variable	Range	Units
$P_{p,i}$	[70, 75, ... 90]	%
t_p	[300, 350, ..., 1000]	ms
T	[15, 25, 48]	$°C$

Table 4 System characterization testing experimental variables

In total, three different tests were conducted for characterization at the temperature setpoints defined in Table 4. Sequences included t_p values less than 300 ms, but the rise in plenum pressure is consistently too insignificant to measure accurately below the 300 ms cutoff. Temperature setpoints represent the nominal and extreme cases. Tests were conducted at temperatures below the 15 $°C$ limit, but sensor precision makes it difficult to post-process the data. This is an artifact of the pressure sensor sensitivity and the main tank pressure at low temperatures. As an example, characterization testing that is run at 0 $°C$ is conducted with a main tank pressure of 15.6 psi. This means that there is only a 3.1 psi difference between the 70% and 90% $P_{p,i}$ pressures. In these conditions, the small pulse lengths do not significantly change the plenum pressure reading until they reach 500 ms. The pressure rises occurring after long

pulse lengths are heavily discretized in increments equivalent to the plenum pressure sensor sensitivity. The 15 $^{\circ}C$ test temperature is the lowest temperature where neither of these issues clearly impacts the post-processed data. Raw data for a characterization test is shown in Figure 9 and Figure 10.

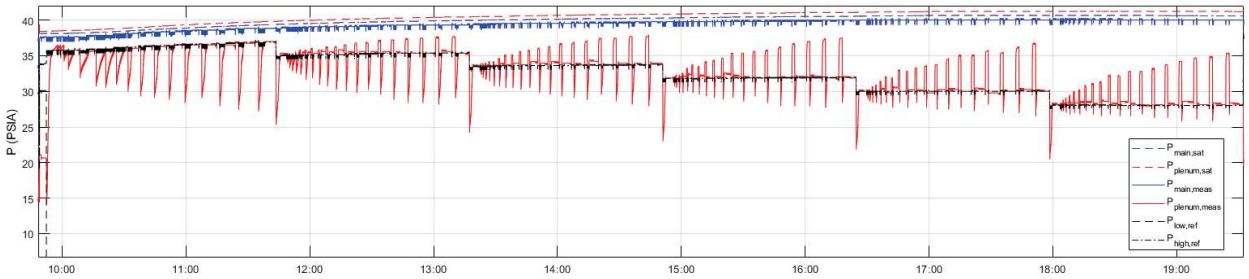

Fig. 9 Ambient system characterization raw data

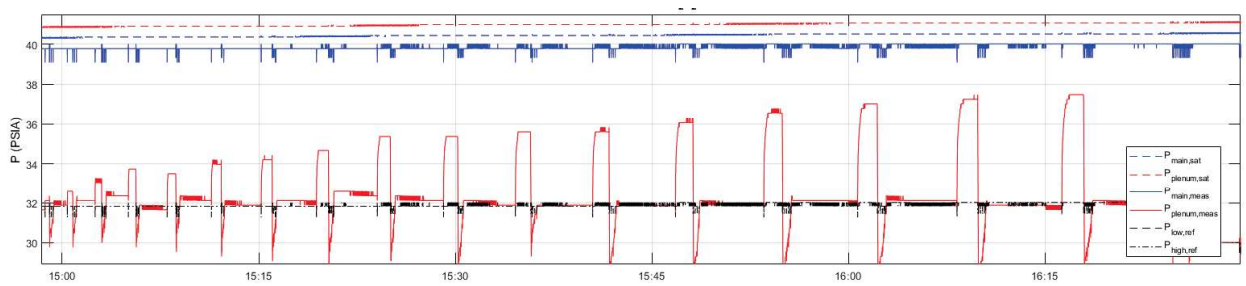

Fig. 10 Snippet of ambient system characterization data - constant initial plenum pressure

This data is post-processed to extract the dependent variable, final plenum pressure ($P_{p,f}$). The raw relationship between refill pulse length, initial plenum pressure, and rise in plenum pressure for the different temperatures are plotted in Figure 11.

Given the processed characterization data, the values corresponding to each individual refill pulse sent during testing were plugged into equation (15) to calculate the parameter c. The next step is to perform regression on the calculated parameter and the collected data to get $f(P_m, P_{p,i}, P_{p,f}, T)$.

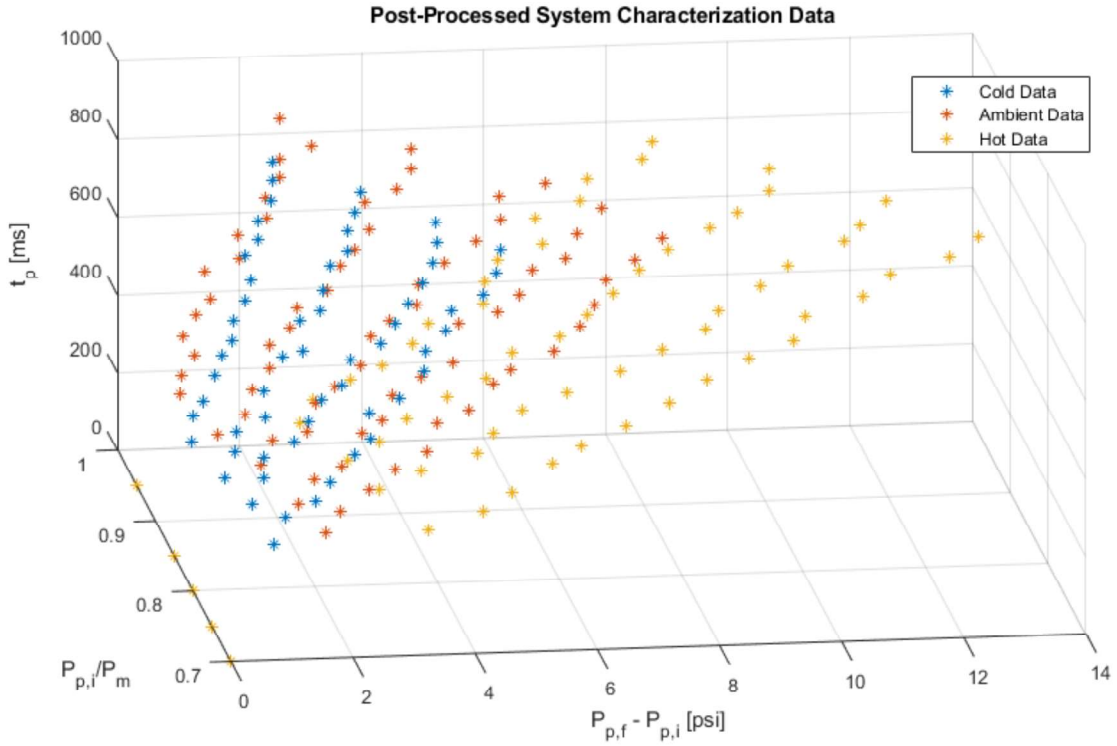

Fig. 11 Post-processed characterization data for the three test temperatures

D. Regression and Model Fit

Second-order regression is performed to get an expression for c. Three regressors were chosen and follow from equation (16). Coefficients, C_i, were found such that the following expression is satisfied

$$c = C_1 R_1^2 + C_2 R_2^2 + C_3 R_3^2 + C_4 R_1 R_2 + C_5 R_1 R_3 + C_6 R_2 R_3 + C_7 R_1 + C_8 R_2 + C_9 R_3 + C_{10} \tag{17}$$

$$R_1 = T \tag{18}$$

$$R_2 = P_m - P_{p,i} \tag{19}$$

$$R_3 = P_{p,f} - P_{p,i} \tag{20}$$

After plugging in all of the experimental data to find the coefficients, C_i, the fit for the data-defined parameter c as a function of known variables had a goodness-of-fit of 0.94. This relationship can now be used in equation (16) to calculate estimates for the pulse time that is needed at any operational state. This function is visualized in Figure 12 with pulse time (t_p) on the z-axis, initial plenum pressure percentage on the x-axis ($\frac{P_{p,i}}{P_m}$), and the difference between initial and final plenum pressures on the y-axis ($P_{p,f} - P_{p,i}$). Each surface represents the operating space for a constant temperature.

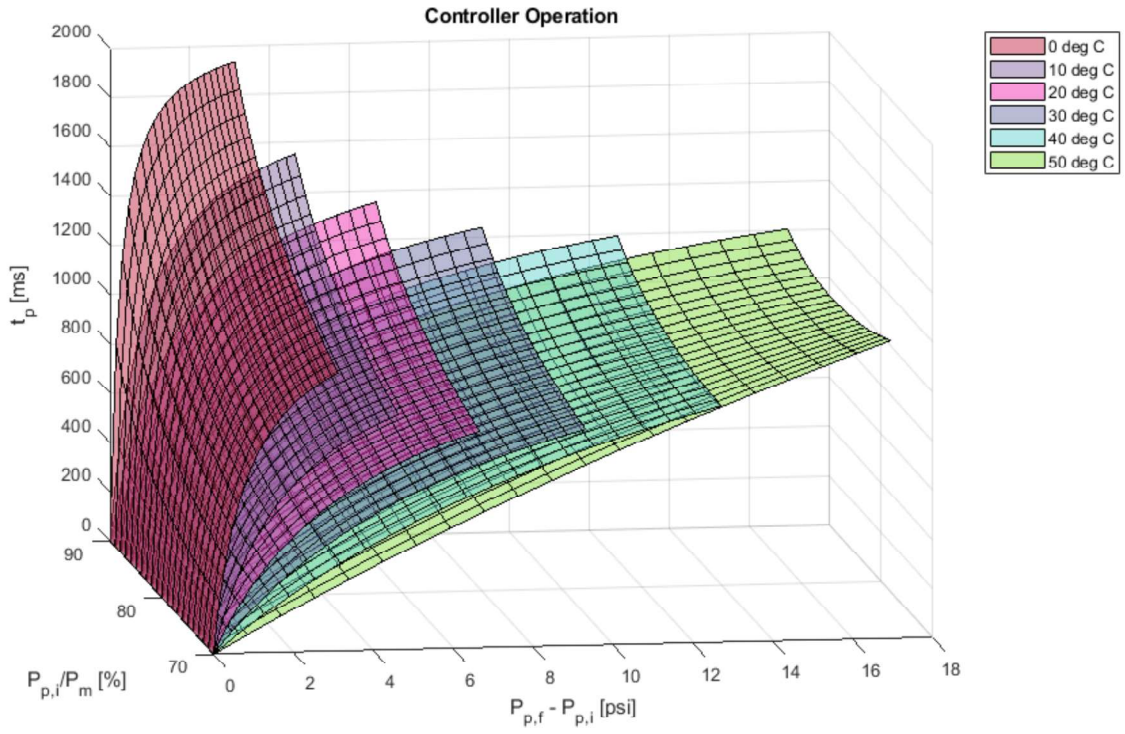

Fig. 12 Pulse time prediction function

The operational limits for this function are defined to avoid the instability that may occur when extrapolating beyond the data-defined model. If any variable in the current state falls outside of these bounds, it is set to the closest limit. A minimum temperature of 0 $°C$ is determined through hardware testing validation of the updated refill strategy. This is a lower temperature than the minimum characterization testing temperature of 15 $°C$, but shows that the use of a first-order flow model enables limited extrapolation beyond the data-defined limits.

	Min.	Max.	Unit
$P_{p,i}$	$0.7P_m$	$0.9P_m$	Pa
$P_{p,f}$ - $P_{p,i}$	0	N/A	Pa
T	0	50	$°C$

V. Refill Validation

The refill strategy is implemented in the firmware for the CGPS system. Logic and timing changed to account for the steady state and pulse time models. Before beginning testing on an EDU or any flight propulsion system, the updated software is validated via unit testing.

A. Software Validation

Embedded software for the CGPS was updated to implement the new refill strategy. Simulated behavior in MATLAB and the onboard controller behavior were checked via a series of unit tests. A serial interface was developed to communicate between MATLAB and an Arduino Mega that runs an updated build of the software. The interface communicates with the CGPS software via the telemetry and command packet structures. A unit testing build of the software is used to set the values of state variables onboard. This allows a user to monitor the behavior of the CGPS software by analyzing the telemetry as it is being commanded into different states. During refill validation, main tank and plenum temperature and pressure values are set and refill commands are sent. Unit tests verify that the refill valve pulse time, t_p, is calculated correctly. They also verify that the controller accurately determines when the plenum pressure has reached a steady state.

The expected system behavior outlined in the Model Development section was all stringently tested. The minimum three second wait for the plenum to reach a steady state was validated. The refill pulse time calculations for both nominal and off-nominal operating conditions were also validated. This includes testing the operational limits that prevent the refill pulse time function from extrapolating beyond the input data. Features were also added as a result of the validation testing. A maximum time to reach a steady state is defined as 50 seconds to avoid any potential hardware failures forcing the system to get stuck in a refill. A 2% dead band is added and validated to ensure that a refill is not triggered when within 2% of the high threshold. This feature prevents the controller from starting another cycle when it is already

sufficiently close to the commanded final plenum pressure.

B. Hardware Testing

Testing is conducted on the same EDU (SunRISE EDU2) that ran through system characterization testing. The first tests were run at an ambient temperature. The tests simulated an extended nozzle firing operation with the EDU in an orientation that forces liquid into the plenum during refills.

After the initial ambient hardware test on SunRISE EDU2, it is determined that the refill strategy needs to be updated to accommodate the physical behavior of the system. It became clear that when the controller is commanding refill pulses immediately after the plenum is depleted, the resulting final plenum pressure would overshoot the high refill bound. A build of the software was implemented to force the controller to wait for three seconds after a refill is commanded before firing a refill pulse. From this testing, it is determined that the plenum exhibits a pressure rebounding effect after firing that is a combined result of liquid in the plenum and heat loss from firing/vaporization. The fixed three second wait time is updated and changed to the steady state determination function. The hardware testing on SunRISE EDU2 was rerun at ambient temperature with the updated strategy and produced results seen in Figure 13.

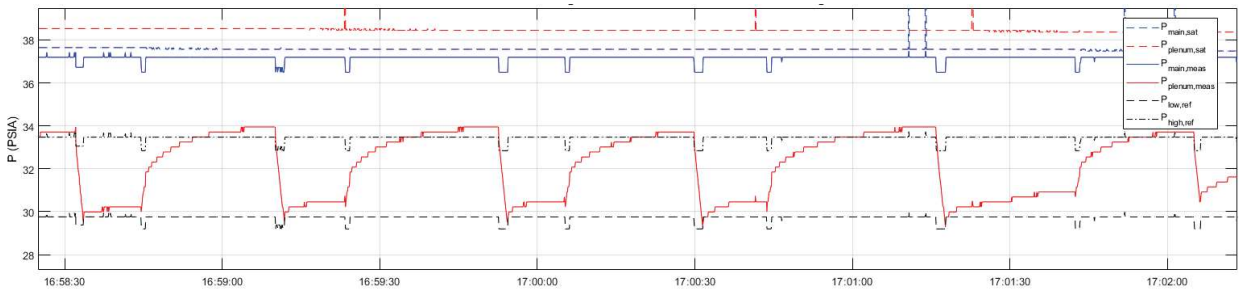

Fig. 13 Snippet of liquid refill validation results on the characterized EDU

The results show that the updated strategy takes approximately 30 seconds for a refill. While this is still an increase compared to the original refill times of 5 to 10 seconds, it is significantly lower than the simple fixed-duty refill cycle. The primary advantage of the updated strategy, though, is the inclusion of logic that actively minimizes the amount of liquid present in the plenum.

Additional hardware tests were run at temperature to validate that the system correctly predicted refill pulse times at both hot and cold temperatures. Hot and cold tests, run at 5 $^{\circ}C$ and 45 $^{\circ}C$, had similar results to the ambient testing seen in Figure 13.

The last validation test run on the EDU is without liquid covering the refill flow path. The orientation of the EDU is inverted to move the gas bubble into the proper position. The results below show a series of gas-only refills and prove that the worst-case liquid assumption allows the system to be operated even when there is no liquid entering the plenum.

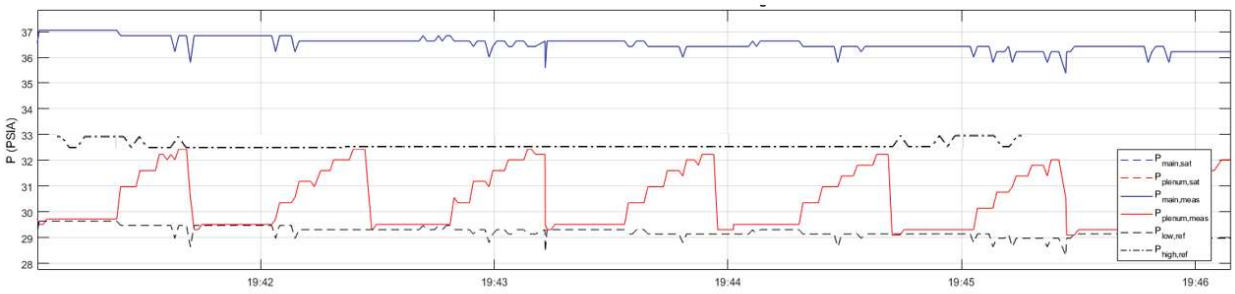

Fig. 14 Snippet of gas refill validation results on original EDU

C. Validations Results

As can be seen in Figure 13, the refill pulses consistently reach the intended final plenum pressure. The strategy compensates for the pressure rebounding effect and is able to make accurate refill pulse time predictions at various different plenum pressures. Nozzle fires are effectively limited to times when the system has clearly reached a steady state final pressure. Figure 13 shows that the intended goals of the update refill strategy development are all met. Similar results can be shown for both low and high system temperatures.

VI. Current Work

Validation testing has been done on the original EDU and various other units. Results vary from unit to unit due to different physical system characteristics. The roughness of the flow paths and the pressure drop across the filters upstream of the valves are examples of variables that cause the deviation in model accuracy [11]. For the updated refill strategy to work sufficiently on units other than the EDU that provided the system characterization data, a scaling function must be added to equation (16).

Results from testing on alternate units had final plenum pressures that were consistently higher than predicted. Increased attenuation of the filters on the characterized EDU is the most likely cause of the overestimates. This is most likely a result of updated cleanliness standards and modified cleaning procedures that have been implemented since the EDU development. Schedule and resource constraints make a full campaign of system characterization on individual units unrealistic. Instead, the overshoot is remedied by performing abbreviated characterization testing on randomly selected units. Consistent results were found across these systems with testing performed at a constant ambient temperature and initial plenum pressure. The ratio between expected and actual final plenum pressures is calculated and a linear scaling function is determined. The results show that predictions for smaller rises in pressure needed to be scaled down, but larger pressure rises were consistent with the EDU results. These findings align with the theory that EDU filter attenuation contributes to overestimates in pulse time calculation. The updated refill function then becomes

$$t_p = f(P_{p,f} - P_{p,i}) \frac{RT\rho_w f(P_m, P_{p,i}, P_{p,f}, T)}{(P_{p,f} - P_{p,i})V} \sqrt{\rho_p (P_m - P_{p,i})} \tag{21}$$

where $f(P_{p,f} - P_{p,i})$ is a linear scaling function that adjusts the pulse time estimate for systems with different filter characteristics. The results of adding this function to the pulse time estimates can be seen during an extending nozzle fire operation of a CGPS flight unit in Figure 15. The update to the refill pulse time prediction has significantly improved the accuracy of the refill strategy.

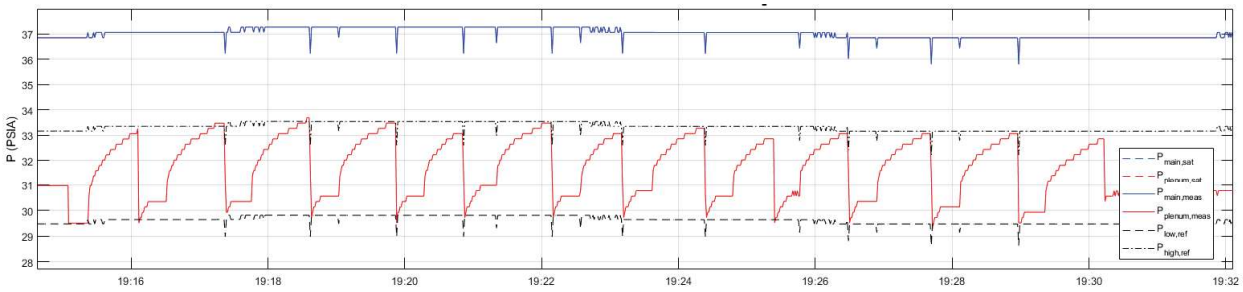

Fig. 15 Snippet of liquid refill validation results on a model adjusted non-EDU unit

VII. Conclusion

The results of an updated refill function for a GLRG CGPS show that systems can now operate with minimized risks associated with liquid in the plenum. Constraining the propulsion system to only fire after a refill has reached a steady state ensures that the majority of the liquid has vaporized. Implementing a data-reinforced model for predicting refill pulse times minimizes the amount of time it takes to refill the plenum. Validation on a software and hardware level was completed and shows that the updated refill strategy performs as intended. Testing of both worst-case liquid refills and best-case gas refills displays the robustness of the refill strategy logic. Finally, updates to the refill pulse time function to account for physical variation across units are performed to ensure the plenum is not consistently overshooting its intended final plenum pressure.

References

[1] Kasper, J., Lazio, J., Romero-Wolf, A., Lux, J., and Neilsen, T., "The Sun Radio Interferometer Space Experiment (SunRISE) Mission Concept," *2019 IEEE Aerospace Conference*, 2019. https://doi.org/10.1109/aero.2019.8742146

[2] Agarwal, R., Oh, B., Fitzpatrick, D., Buynovskiy, A., Lowe, S., Lisy, C., Kriezis, A., Lan, B., Lee, Z., Thomas, A., Wallace, B., Costantino, E., Miner, G., Thayer, J., D'Amico, S., Lemmer, K., Lohmeyer, W., and Palo, S., "Coordinating Development of the SWARM-EX CubeSat Swarm Across Multiple Institutions," *Small Satellite Conference*, 2021. URL https://digitalcommons.usu.edu/smallsat/2021/all2021/230/

[3] Lightsey, E. G., Arunkumar, E., Kimmel, E., Kolhof, M., Paletta, A., Rawson, W., Selvamurugan, S., Sample, J., Guffanti, T., Bell, T., Koenig, A., Amico, S., Park, H., Rabin, D., Daw, A., Chamberlin, P., and Kamalabadi, F., "Concept of Operations for the VISORS Mission: A Two Satellite CubeSat Formation Flying Mission," , 2022. URL https://ssdl.gatech.edu/sites/default/files/ssdl-files/papers/conferencePapers/AAS_202202_Visors.pdf

[4] Stevenson, T., "Development of Multi-Functional Structures for Small Satellites," , 2018. URL https://ssdl.gatech.edu/sites/default/files/ssdl-files/papers/phdTheses/StevensonT-Thesis.pdf

[5] Lightsey, E. G., Stevenson, T., and Sorgenfrei, M., "Development and Testing of a 3-D-Printed Cold Gas Thruster for an Interplanetary CubeSat," *Proceedings of the IEEE*, Vol. 106, 2018, pp. 379–390. https://doi.org/10.1109/jproc.2018.2799898

[6] Shirazi, K., and Lightsey, E. G., "Integration and Testing of a 2U Cold-Gas Propulsion System for the SunRISE Mission," , 2022. URL https://ssdl.gatech.edu/sites/default/files/ssdl-files/papers/mastersProjects/ShiraziK-8900.pdf

[7] Hart, S., and Lightsey, E. G., "Design of the VISORS and SWARM-EX Propulsion Systems," , 2022. URL https://ssdl.gatech.edu/sites/default/files/ssdl-files/papers/mastersProjects/8900_hart_draft2.pdf

[8] Skidmore, L., and Lightsey, E. G., "Design of a Cold Gas Propulsion System for the SunRISE Mission," , 2021. URL https://www.ssdl.gatech.edu/sites/default/files/ssdl-files/papers/mastersProjects/Skidmore_AE_8900.pdf

[9] Bell, I. H., Wronski, J., Quoilin, S., and Lemort, V., "Pure and Pseudo-pure Fluid Thermophysical Property Evaluation and the Open-Source Thermophysical Property Library CoolProp," *Industrial Engineering Chemistry Research*, Vol. 53, 2014, pp. 2498–2508. https://doi.org/10.1021/ie4033999

[10] Collicott, S. H., Beckman, E. A., and Srikanth, P., "Conformal Tanks: Small-Sat Propellant Management Technology," *AIAA Propulsion and Energy 2019 Forum*, 2019. https://doi.org/10.2514/6.2019-3874

[11] Valve, C., *Flow of Fluids through Valves, Fittings, and Pipes*, Vervante, 1998.